

# Universality of Non-equilibrium Fluctuations in Strongly Correlated Quantum Liquids

Meydi Ferrier<sup>1,2</sup>, Tomonori Arakawa<sup>1</sup>, Tokuro Hata<sup>1</sup>, Ryo Fujiwara<sup>1</sup>, Raphaëlle Delagrangé<sup>2</sup>, Raphaël Weil<sup>2</sup>, Richard Deblock<sup>2</sup>, Rui Sakano<sup>3</sup>, Akira Oguri<sup>4</sup>, Kensuke Kobayashi<sup>1</sup>

<sup>1</sup>*Department of Physics, Graduate School of Science, Osaka University, 1-1 Machikaneyama, Toyonaka, 560-0043 Osaka, Japan*

<sup>2</sup>*Laboratoire de Physique des Solides, CNRS, Univ. Paris-Sud, Université Paris Saclay, 91405 Orsay Cedex, France*

<sup>3</sup>*The Institute for Solid State Physics, The University of Tokyo, Kashiwa, Chiba 277-8581, Japan*

<sup>4</sup>*Department of Physics, Osaka City University, Sumiyoshi-ku, Osaka 558-8585, Japan*

Interacting quantum many-body systems constitute a fascinating playground for researchers since they form quantum liquids with correlated ground states and low-lying excitations, which exhibit universal behaviour<sup>1</sup>. In fermionic systems, such quantum liquids are realized in helium-3 liquid, heavy fermion systems<sup>1</sup>, neutron stars and cold gases<sup>2</sup>. Their properties in the linear-response regime have been successfully described by the theory of Fermi liquids<sup>1</sup>. However, non-equilibrium properties beyond this regime have still to be established and remain a key issue of many-body physics. Here, we show a precise experimental demonstration of Landau Fermi-liquid theory extended to the non-equilibrium regime in a 0-D system. Combining transport and ultra-sensitive current noise measurements, we have unambiguously identified the  $SU(2)$ <sup>3</sup> and  $SU(4)$ <sup>4-8</sup> symmetries of quantum liquid in a carbon

nanotube tuned in the universal Kondo regime. We find that, while the electronic transport is well described by the free quasi-particle picture around equilibrium <sup>9</sup>, a two-particle scattering process due to residual interaction shows up in the non-equilibrium regime <sup>8,10–17</sup>. By using the extended Fermi-liquid theory, we obtain the interaction parameter “Wilson ratio”<sup>18</sup>  $R = 1.9 \pm 0.1$  for SU(2) and  $R = 1.35 \pm 0.1$  for SU(4) as well as the corresponding effective charges, characterizing the quantum liquid behaviour. This result, in perfect agreement with theory<sup>10,12–15</sup>, provides a strong quantitative experimental background for further developments of the many-body physics. Moreover, we discovered a new scaling law for the effective charge, signalling as-yet-unknown universality in the non-equilibrium regime. Our method to address quantum liquids through their non-equilibrium noise paves a new road to tackle the exotic nature of quantum liquids out-of-equilibrium in various physical systems <sup>19</sup>.

The Kondo effect <sup>20</sup> is a typical example of quantum many body effect, where a localised spin is screened by the surrounding conduction electrons at low temperature to form a unique correlated ground state. The Kondo state is well described by the Fermi-liquid theory at equilibrium <sup>1,9</sup>, which makes it an ideal test-bed to go beyond. To unveil the universal behaviour of non-equilibrium Fermi-liquid <sup>11</sup>, we have used the current fluctuations or shot noise in a Kondo-correlated nanotube quantum dot<sup>19</sup>.

When electrons are transmitted through this system, the scattering induces the shot noise, which sensitively reflects the nature of the quasi-particles<sup>21</sup>, as shown in the upper panel of Fig.1a. A remarkable prediction of the non-equilibrium Fermi-liquid theory is that the residual interaction

creates an additional scattering of two particles which enhances the noise (see the lower panel of Fig.1a)<sup>10,12–15</sup>. This two-particle scattering is characterized by an effective charge  $e^*$  larger than  $e$  (electron charge). This value, closely related to the Wilson ratio, is universal for the Fermi-liquid in the Kondo regime since it only depends on the symmetry group of the system<sup>13–15</sup>. While some aspects of the Kondo-associated noise were reported<sup>8,16,17</sup>, a rigorous, self-consistent treatment in a regime where universal results apply is at the core of the present work. Actually, by tuning a nanotube quantum dot from the spin degenerate SU(2) Kondo regime to the spin-orbit degenerate SU(4) one, the noise is proven to contain distinct signatures of these two symmetries, confirming theoretical developments of Fermi-liquid theory out of equilibrium.

In our experiment, we measured the conductance and current noise through a carbon nanotube quantum dot grown by chemical vapour deposition<sup>22</sup> on an oxidized undoped silicon wafer and connected with a Pd (6 nm)/Al(70 nm) bilayer. The distance between the contacts is 400 nm and a side gate electrode is deposited to tune the potential of the quantum dot (see Fig 1b). To measure accurately the shot noise, our sample is connected to a resonant (2.58 MHz) LC circuit. The signal across this resonator is measured with a home-made cryogenic low-noise amplifier<sup>23</sup>. Figure 2a presents the image-plot of the differential conductance of the sample ( $G$ ) at temperature  $T = 16$  mK as a function of source-drain voltage ( $V_{sd}$ ) and gate voltage ( $V_g$ ). This stability diagram shows the four-fold degenerated Coulomb diamonds specific to carbon nanotubes. The spectrum consists in successive four-electron shells. We note  $N = 0, 1, 2, 3$  the number of electrons in the last shell. Remarkably, the SU(2) and SU(4) Kondo ridges<sup>6</sup> emerge as horizontal bright regions (high conductance) at  $V_{sd} = 0$ .

For the moment, we concentrate on the SU(2) region. A cut of the conductance at  $V_{sd} = 0$  is represented in the upper panel of Fig. 2b. Two Kondo ridges appear as plateaux where  $G$  is maximum for the filling  $N = 1$  (ridge A) and  $N = 3$  (ridge B), whereas  $G$  decreases to almost zero for even  $N$ . In addition, the ridge B is flat and the unitary limit is achieved: the conductance reaches the quantum of conductance  $G_Q = 2e^2/h$  which is a signature of perfect Kondo effect in a dot with symmetric coupling to the leads. The Kondo temperature ( $T_K$ ) is  $1.6 \pm 0.05$  K in the centre of this ridge (see supplementary).

The current noise  $S_i$  as well as  $G$  are plotted on the Figs. 2c and 2d for  $N = 2$  and  $N = 3$  as a function of the source-drain current  $I_{sd}$ . Outside the Kondo ridge ( $N = 2$ )  $S_i$  is linear with  $|I_{sd}|$ , whereas on the ridge the shot noise is flat around  $I_{sd} = 0$  and enhanced at high current when the energy of incoming electrons approaches a fraction of  $T_K$ . At high voltage ( $eV_{sd} \gg k_B T_K$ ), a linear behaviour is recovered with  $S_i = 2e|I_{sd}|$ . To analyse the low energy properties, we have extracted the Fano factor ( $F$ ) which is defined as:  $S_i = 2eF|I_{sd}|$  from a linear fit at low current.  $F$  varies approximately from zero on the Kondo ridge to  $F = 1$  outside as shown in the bottom panel of Fig.2b. Indeed at very low energy, as the free quasi-particle picture of the Fermi-liquid theory teaches us, the conductance and the noise for a multichannel conductor can be written as a function of transmission  $T_i$  for each channel  $i = 1, 2, 3 \dots$  <sup>21</sup>:

$$G = G_Q \sum T_i \quad \text{and} \quad F = \frac{G_Q}{G} \sum T_i(1 - T_i). \quad (1)$$

For the SU(2) symmetry, transport occurs through one single channel yielding  $G = G_Q T_1$  and  $F = 1 - T_1$ . On the Kondo ridge, the conductance is  $G = G_Q$  yielding  $T_1 = 1$  and  $F = 1 - T_1 = 0$ . This is a direct signature of the Kondo resonance which allows a perfect transmission and thus no

partition of quasi-particles near equilibrium. In the Coulomb blockade regime for even  $N$ , the transport is blocked ( $T_1 \ll 1$ ) yielding  $F \approx 1$  indicating that transport occurs through tunnelling events resulting in a conventional Poissonian noise.

At higher voltages ( $0 < eV_{sd} \leq k_B T_K/2$ ) we concentrate only on the non-linear terms for current and noise by subtracting the linear part. We defined  $S_K = S_i - 2eF|I_{sd}|$  and the backscattered current  $I_K = G(0)V_{sd} - I_{sd}$ <sup>10,13</sup>. These quantities are related through the effective charge<sup>10,12,13,24</sup>  $e^*$ :

$$S_K = 2e^*|I_K|. \quad (2)$$

This effective charge does not imply an exotic charge as in the quantum Hall regime but it is related to the probability that one particle or two particles are backscattered in the Fermi-liquid. Figures 3a and 3b show the evolution of the conductance on ridge B as a function of magnetic field  $B$  and the corresponding noise  $S_K$  as a function of  $I_K$ , respectively. The temperature dependence is analysed in details in the supplementary. The effective charge is directly given by the slope at low current  $I_K$  ( $eV_{sd} < k_B T_K$ ) yielding for the lowest field and temperature  $e^*/e = 1.7 \pm 0.1$ . This result is in good agreement with theory<sup>10,12</sup>, which predicts  $e^*/e = 5/3 \approx 1.67$  corresponding to equal probabilities for one or two-particle scattering. Figure 3c represents the evolution of  $e^*$  with magnetic field and temperature. On this graph  $e^*$  is represented as a function of the reduced scales  $\frac{T}{T_K}$  for temperature or  $\frac{g\mu_B B}{2k_B T_K}$  for the field where  $g = 2$  is the Landé factor and  $\mu_B$  the Bohr magneton (see supplementary). All the data points seem to fall on the same curve suggesting that  $e^*$  obeys a logarithmic scaling law which has not yet been predicted.

The Wilson ratio  $R$  has been extracted from the formula<sup>12,15</sup>:

$$\frac{e^*}{e} = \frac{1 + 9(n-1)(R-1)^2}{1 + 5(n-1)(R-1)^2} \quad (3)$$

where  $n$  characterizes the symmetry group  $SU(n)$  of the Kondo state. This number  $R$  is directly related to the ratio  $U/\Gamma$  with  $U$  the charging energy of the quantum dot and  $\Gamma$  the coupling to the electrodes. It reflects the strength of the interaction in the Fermi-liquid and is the only parameter to characterize the system, going from  $R = 1$  in the non interacting case ( $U = 0$ ) to  $R = 2$  in the strong  $SU(2)$  Kondo limit ( $U \rightarrow \infty$ ) (see Fig.3d). Our value for  $e^*$  yields  $R = 1.95 \pm 0.1$  ensuring strong interactions and thus universal regime.

For consistency,  $R$  was independently extracted by fitting the evolution of conductance with  $B, V_{sd}$  and  $T$  at low excitation (see supplementary) without any assumption on  $T_K$ . This result,  $R = 1.95 \pm 0.1$ , perfectly agrees with the value extracted from  $e^*$ . Finally, from the dependence of  $T_K$  with gate voltage, we have independently extracted the values  $U = 6 \pm 0.5$  meV and  $\Gamma = 1.8 \pm 0.2$  meV. This consistency is illustrated in Fig.3d where the two independent values for  $R$  and  $U/\Gamma$  cross on the theoretical curve.

The effect of asymmetric lead-dot coupling was tested on the ridge A where  $G = 0.85 G_Q$ . Asymmetry is defined by the factor  $\delta$  such that  $G(0) = (1 - \delta)G_Q$ . We have measured an effective charge  $e^*/e = 1.2 \pm 0.08$  in good agreement with Ref. [14] which predicts  $\frac{e^*}{e} = \frac{5}{3} - \frac{8}{3}\delta = 1.26$ .

Now, what can we learn from the  $SU(4)$  symmetry emerging in the right part of Fig. 2a? A zoom is plotted in the upper panel of Fig.4a and the cross-section is displayed in the middle part.

Since spin and orbital degrees of freedom are degenerated, two channels contribute to transport and Kondo resonance emerges at every filling factors  $N = 1, 2$  and  $3$  electrons<sup>4-7</sup>. At odd filling, the channels are half transmitted ( $T_1 = T_2 = 0.5$ ) yielding the same conductance  $G_Q$  as in the SU(2) symmetry. However for  $N = 2$ , current is transmitted through two perfect channels ( $T_1 = T_2 = 1$ ) increasing the conductance up to  $G = 2 G_Q$ . In this region the conductance hardly depends on temperature up to 800 mK reflecting a large  $T_K$  as expected for the SU(4) symmetry<sup>25</sup>. This is confirmed by the full width of the curve  $G(V_{sd})$  which gives  $T_K \approx 11$  K for  $N = 2$  and  $T_K \approx 17$  K for  $N = 1$  or  $3$ .

The first result to emphasize is that the linear part of the current noise is qualitatively different from SU(2) and is a powerful experimental tool to distinguish the two symmetries<sup>14,19</sup>. The upper part of Fig. 4b represents the conductance at  $N = 3$  for SU(2) and SU(4) as a function of the rescaled voltage  $eV_{sd}/k_B T_K$ . The two curves are barely distinguishable. However the current noise displayed on the lower part of Fig. 4b is qualitatively different since it is almost zero for the SU(2) symmetry whereas it is linear with  $|I_{sd}|$  for SU(4). The linear noise is one order of magnitude stronger for SU(4) than for SU(2). Indeed, the Fano factor for two channels such that  $T_1 = T_2 = 0.5$  is  $F = 0.5$  for the SU(4) symmetry whereas for SU(2) a single channel with  $T_1 = 1$  yields  $F = 0$ . The complete evolution of  $F$  is summarized in the lower part of Fig. 4a. It changes from  $F \approx 1$  outside the Kondo ridge to  $F = 0.5$  for  $N = 1$  and  $3$  and reaches  $F = 0.07$  for  $N = 2$ . This confirms that in the  $N = 2$  SU(4) case, transport takes place through two almost perfect channels ( $T_1 = T_2 = 1$ ) without partition yielding  $F \approx 0$ .

Finally we discuss  $e^*$  and  $R$  for the SU(4) symmetry at half filling ( $N = 2$ ).  $S_K$  and  $I_K$  have been computed by using the same procedure as explained for SU(2). The result, displayed on Fig. 4c, gives  $e^*/e = 1.45 \pm 0.1$  and  $R = 1.35 \pm 0.1$  from Eqn (3). The decreasing value for  $R$  and  $e^*$  reflects the increasing number of degenerated states. When degeneracy increases, electrons correlations become weaker and the non-interacting value is recovered for SU( $n$ ) when  $n \rightarrow \infty$ . The values for  $e^*$  and  $R$  are in good agreement with Refs. [14, 15] (also see Fig. 3d) confirming that non-equilibrium Fermi-liquid theory can be extended to more exotic classes of Fermi-liquids.

Our experimental results emphasize three important points for the theory of Fermi-liquids. First, in the linear regime they can be described as free quasi-particles as the spirit of the theory teaches us. This allows to clearly distinguish the different symmetry class of Fermi-liquid through shot noise measurements, while it is hardly possible from the conductance. Second, by probing the nonlinear noise, we have shown that out-of-equilibrium the residual interaction between quasi-particles shows up and creates a peculiar two-particle scattering, which bares the signature of the correlated nature of quantum liquids. Finally the newly discovered out-of-equilibrium scaling law should trigger theoretical developments to deepen our understanding of universal behaviours in these liquids.

## Methods

The nanotube has been grown by a very low pressure CVD technique <sup>22</sup>. We have deposited Fe catalyst by electron beam lithography on a non-doped silicon substrate and exposed it to 10 mbar of acetylene during 9 s at a temperature of 900 °C. Nanotubes were located by SEM and contacts were



designed by standard e-beam lithography. The metallic bilayer (6 nm Pd/70 nm Al) is deposited on the contacts by e-gun evaporation. An in-plane magnetic field  $B = 0.08$  T is applied to suppress the superconductivity of the contacts.

The shot noise is measured with a resonant set-up<sup>23</sup>. The sample is connected to a LC circuit with a resonance frequency of 2.58 MHz thermalized on the mixing chamber of the dilution fridge. The power spectral density of the noise is obtained through the following procedure: amplifying the noise signal with a home-made amplifier fixed on the 1K pot of the dilution fridge and again at room-temperature, taking the time-domain signal by a digitizer (National Instruments PCI-5922) and performing the fast Fourier transformation of the data. The current noise of the sample is then extracted from the fit of the shape of the resonance in the frequency domain.

## References

1. Mahan, G. D. *Many-Particle Physics* (Plenum Press, New York, 1990).
2. Bloch, I., Dalibard, J. & Nascimbène, S. Quantum simulations with ultracold quantum gases. *Nat. Phys.* **8**, 267–276 (2012).
3. van der Wiel, W. G. *et al.* The Kondo effect in the unitary limit. *Science* **289**, 2105–2108 (2000).
4. Jarillo-herrero, P. *et al.* Orbital Kondo effect in carbon nanotubes. *Nature* **434**, 484–488 (2005).

5. Makarovski, A., Zhukov, A., Liu, J. & Finkelstein, G. SU(2) and SU(4) Kondo effects in carbon nanotube quantum dots. *Phys. Rev. B* **75**, 241407 (2007).
6. Cleuziou, J. P., NGuyen, N. G., Florens, S. & Wernsdorfer, W. Interplay of the Kondo effect and strong spin-orbit coupling in multihole ultraclean carbon nanotubes. *Phys. Rev. Lett.* **111**, 136803 (2013).
7. Schmid, D. R. *et al.* Broken SU(4) symmetry in a Kondo-correlated carbon nanotube. *Phys. Rev. B* **91**, 155435 (2015).
8. Delattre, T. *et al.* Noisy Kondo impurities. *Nat. Phys.* **5**, 208–212 (2009).
9. Nozières, P. A ” Fermi-Liquid ” description of the Kondo problem at low temperatures. *J. Low Temp. Phys.* **17**, 31–42 (1974).
10. Sela, E., Oreg, Y., von Oppen, F. & Koch, J. Fractional shot noise in the Kondo regime. *Phys. Rev. Lett.* **97**, 086601 (2006).
11. Oguri, A. Fermi liquid theory for the nonequilibrium Kondo effect at low bias voltages. *J. Phys. Soc. Japan* **74**, 110–117 (2005).
12. Gogolin, A. O. & Komnik, A. Full counting statistics for the Kondo dot in the unitary limit. *Phys. Rev. Lett.* **97**, 016602 (2006).
13. Mora, C., Leyronas, X. & Regnault, N. Current noise through a Kondo quantum dot in a SU(N) Fermi liquid state. *Phys. Rev. Lett.* **100**, 036604 (2008).

14. Mora, C., Vitushinsky, P., Leyronas, X., Clerk, A. & Le Hur, K. Theory of nonequilibrium transport in the SU(N) Kondo regime. *Phys. Rev. B* **80**, 155322 (2009).
15. Sakano, R., Fujii, T. & Oguri, A. Kondo crossover in shot noise of a single quantum dot with orbital degeneracy. *Phys. Rev. B* **83**, 075440 (2011).
16. Zarchin, O., Zaffalon, M., Heiblum, M., Mahalu, D. & Umansky, V. Two-electron bunching in transport through a quantum dot induced by Kondo correlations. *Phys. Rev. B* **77**, 241303 (2008).
17. Yamauchi, Y. *et al.* Evolution of the Kondo effect in a quantum dot probed by shot noise. *Phys. Rev. Lett.* **106**, 176601 (2011).
18. Wilson, K. G. The renormalization group: Critical phenomena and the Kondo problem. *Rev. Mod. Phys.* **47**, 773–840 (1975).
19. Egger, R. What the noise is all about. *Nat. Phys.* **5**, 175–176 (2009).
20. Kondo, J. Resistance minimum in dilute magnetic alloys. *Prog. Theor. Phys.* **32**, 37–49 (1964).
21. Blanter, Y. M. & Büttiker, M. Shot noise in mesoscopic conductors. *Phys. Rep.* **336**, 1–166 (2000).
22. Kasumov, Y. *et al.* CVD growth of carbon nanotubes at very low pressure of acetylene. *Appl. Phys. A* **88**, 687–691 (2007).
23. Arakawa, T., Nishihara, Y., Maeda, M., Norimoto, S. & Kobayashi, K. Cryogenic amplifier for shot noise measurement at 20 mK. *Appl. Phys. Lett.* **103**, 172104 (2013).

24. Sakano, R., Oguri, A., Kato, T. & Tarucha, S. Full counting statistics for SU(N) impurity Anderson model. *Phys. Rev. B* **83**, 241301 (2011).
25. Galpin, M. R., Logan, D. E. & Krishnamurthy, H. R. Quantum phase transition in capacitively coupled double quantum dots. *Phys. Rev. Lett.* **94**, 186406 (2005).

**Correspondence** Correspondence and requests for materials should be addressed to M. Ferrier. (email: meydi.ferrier@u-psud.fr) or K. Kobayashi. (email: kensuke@meso.phys.sci.osaka-u.ac.jp)

**Acknowledgements** We appreciate discussions with H. Bouchiat and R. Yoshii. This work was partially supported by a Grant-in-Aid for Scientific Research (S) (No. 26220711), JSPS KAKENHI (No. 26400319, 25800174 and 15K17680), Invitation Fellowships for Research in Japan from JSPS, Grant-in-Aid for Scientific Research on Innovative Areas "Fluctuation & Structure" (No. 25103003) and "Topological Materials Science" (KAKENHI Grant No. 15H05854), the Program for Promoting the Enhancement of Research Universities from MEXT, and Yazaki Memorial Foundation for Science and Technology, the French program ANR DYMESYS (ANR2011-IS04-001-01) and ANR MASH (ANR-12-BS04-0016). KK acknowledges the stimulated discussion in the meeting of the Cooperative Research Project of RIEC, Tohoku University.

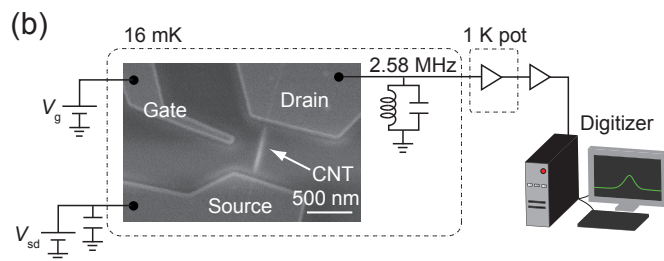
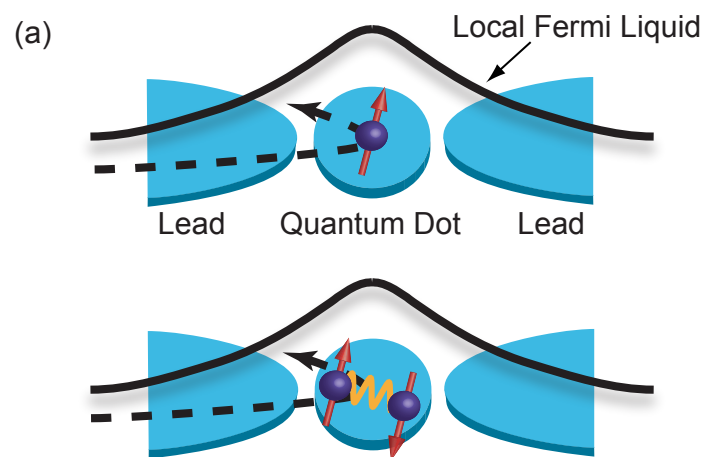


**Figure 1 Illustration of the interaction effect in the quantum liquid and design of the sample.** **a)** Scheme of a quantum dot coupled to two leads. If a single spin is confined on the dot and the coupling with the leads is strong enough, the Kondo effect occurs. The full black line represents the extension of the Kondo state where electrons form a strongly correlated Fermi-liquid. Our work consists in a collision experiment. We inject electrons through this state and observe via the current fluctuations which quasi-particles are backscattered. Upper part) At low energy, this liquid can be understood as an ensemble of non-interacting quasi-particles. During a collision, only single quasi-particles are excited and backscattered by an incoming electron. Lower part) At higher energy the incoming electron can excite two quasi-particles of the Fermi-liquid through the residual interaction between quasi-particles (orange meander line). The scattered current consists then of single or double quasi-particles shots which increase the current fluctuations. The effective charge  $e^*$  is a measure of the probability for these two processes. The Wilson ratio  $R$  quantifies the strength of the interaction between two quasi-particles. **b)** Sample and experimental set-up. SEM image of a carbon nanotube connected to metallic leads on a silicon wafer. It is connected to the current and noise measurement set-up through a resonant circuit fixed on the mixing chamber of the dilution fridge. The gate voltage  $V_g$  tunes the number of electrons ( $N$ ) in the dot and the coupling between dot and leads.

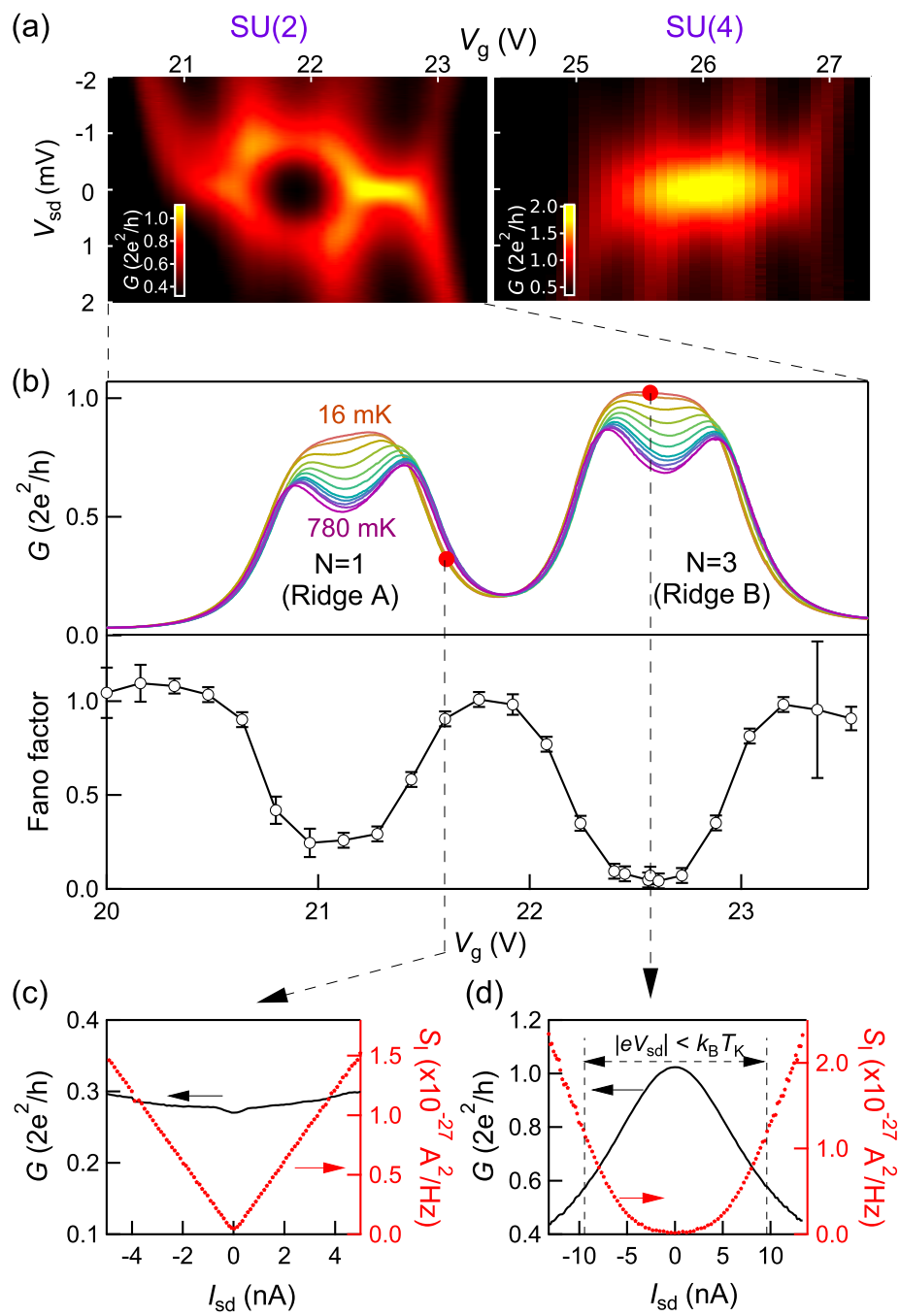


**Figure 2**

**Figure 2: Stability diagram and shot noise for the SU(2) Kondo effect at  $T = 16$  mK.**

**a)** 2D plot of the conductance as a function of  $V_{sd}$  and  $V_g$ . Kondo ridges appear as bright horizontal lines for  $V_{sd} = 0$ . In the SU(2) region two ridges show up for  $N = 1$  and  $N = 3$  electrons. For SU(4) the Kondo ridge exists for  $N = 1, 2$  and 3 electrons. Note that the conductance scale is  $2e^2/h$  for SU(2) whereas it is  $2 \times 2e^2/h$  for SU(4). An in-plane magnetic field of 0.08 T is applied to suppress superconductivity in the contacts.

**b) Upper panel:** Cross-sections of the conductance of the SU(2) Kondo region at zero bias as a function of  $V_g$  for different temperatures. Two Kondo ridges A and B are clearly visible. **Lower panel:** Fano factor extracted from the linear part of the current noise in the regime  $eV_{sd} \ll k_B T_K$  ( $I_{sd} \leq 5$  nA) using the definition  $S_i = 2eF|I_{sd}|$ . **c)** Conductance (black line) and noise (red dots) as a function of  $I_{sd}$  for the blockaded region ( $N = 2$ ). The noise is linear with  $|I_{sd}|$  with a slope around  $2e$ . Outside the Kondo ridge due to the very small transmission, the quantum dot is close to the tunneling regime characterized by a full poissonian noise with  $F = 1$ . **d)** Conductance (black line) and noise (red dots) as a function of  $I_{sd}$  on the Kondo ridge ( $N = 3$ ). The slope of  $S_i$  around  $I_{sd} = 0$  is almost 0 due to the perfect transmission ( $F = 0.06$ ).



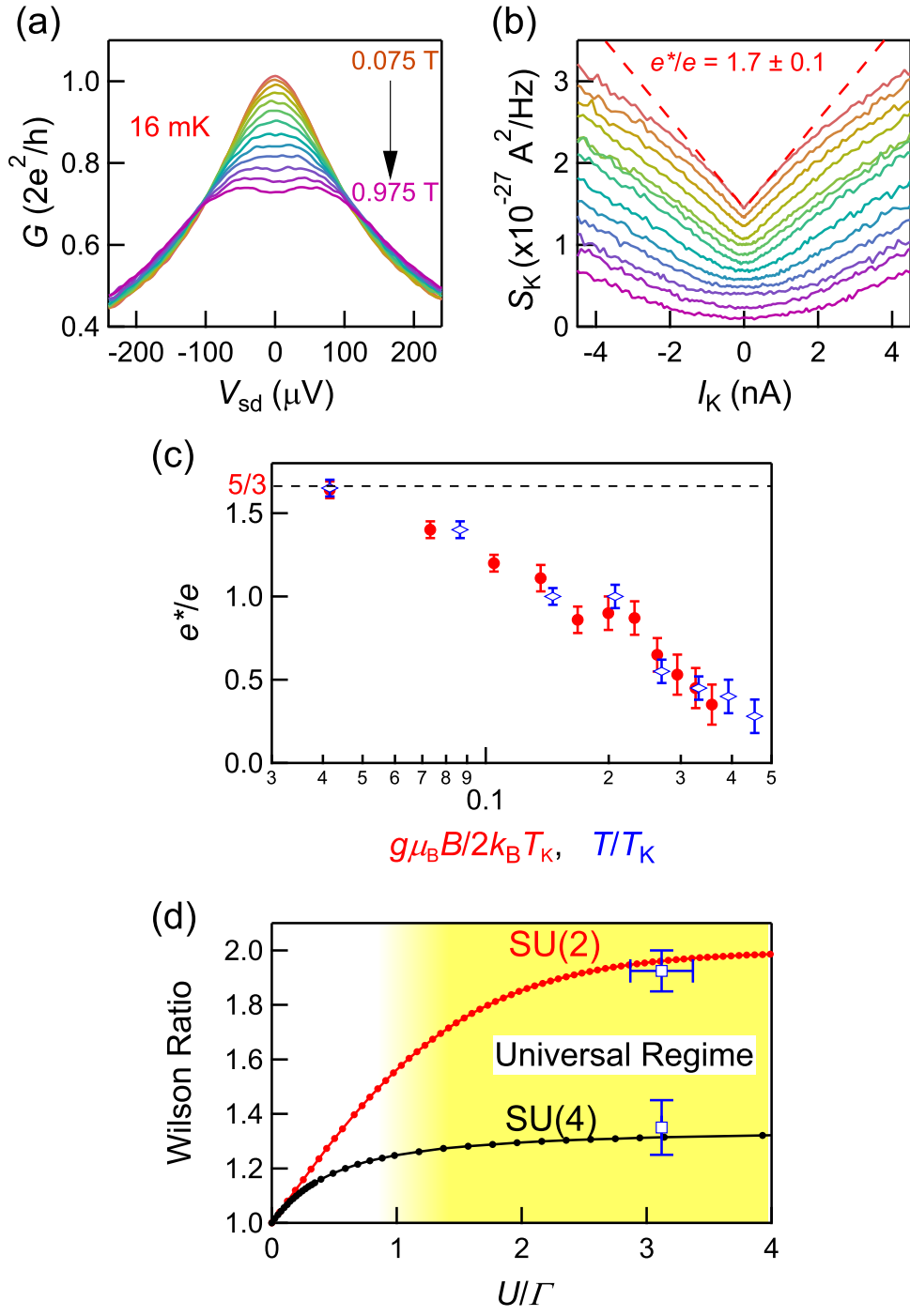


Figure 3

**Figure 3: Evolution of Kondo correlations with magnetic field and temperature.** **a)** Evolution of the differential conductance from 0.075 T to 0.975 T with a step of 0.075 T. **b)** Kondo excess current noise  $S_K$  as a function of backscattering current  $I_K$  (see text for definition) for the same fields. The effective charge  $e^*$  is extracted from the slope  $\frac{S_K}{2eI_K}$  at low current. The red dotted-line shows result of the linear fit yielding  $e^*/e = 1.7 \pm 0.1$ . The curves are shifted for clarity. **c)** Effective charge as a function of  $T/T_K$  and  $\frac{g\mu_B B}{2k_B T_K}$  in a semi-log plot. Both can be described by the same line which is a signature of a scaling law for  $e^*(T, B)$  and suggest a logarithmic behaviour. **d)** Wilson ratio as a function of  $U/\Gamma$  calculated with the formula from [15]. For SU(2), vertical error bars represent the value for  $R$  extracted from  $e^*$  and from the scaling analysis of the conductance shown in the supplementary. Horizontal error bar represents the value for  $U/\Gamma$  extracted independently from the fit of Kondo temperature shown in the supplementary. The crossing on the theoretical curve shows the agreement of our measurement with the extension of Fermi-liquid theory out of equilibrium. For SU(4), the value of  $R$  is extracted from  $e^*$ . The yellow part of the graph represents the region of universality : all the properties depend on a single parameter  $T_K$  for a given symmetry group <sup>11</sup>.

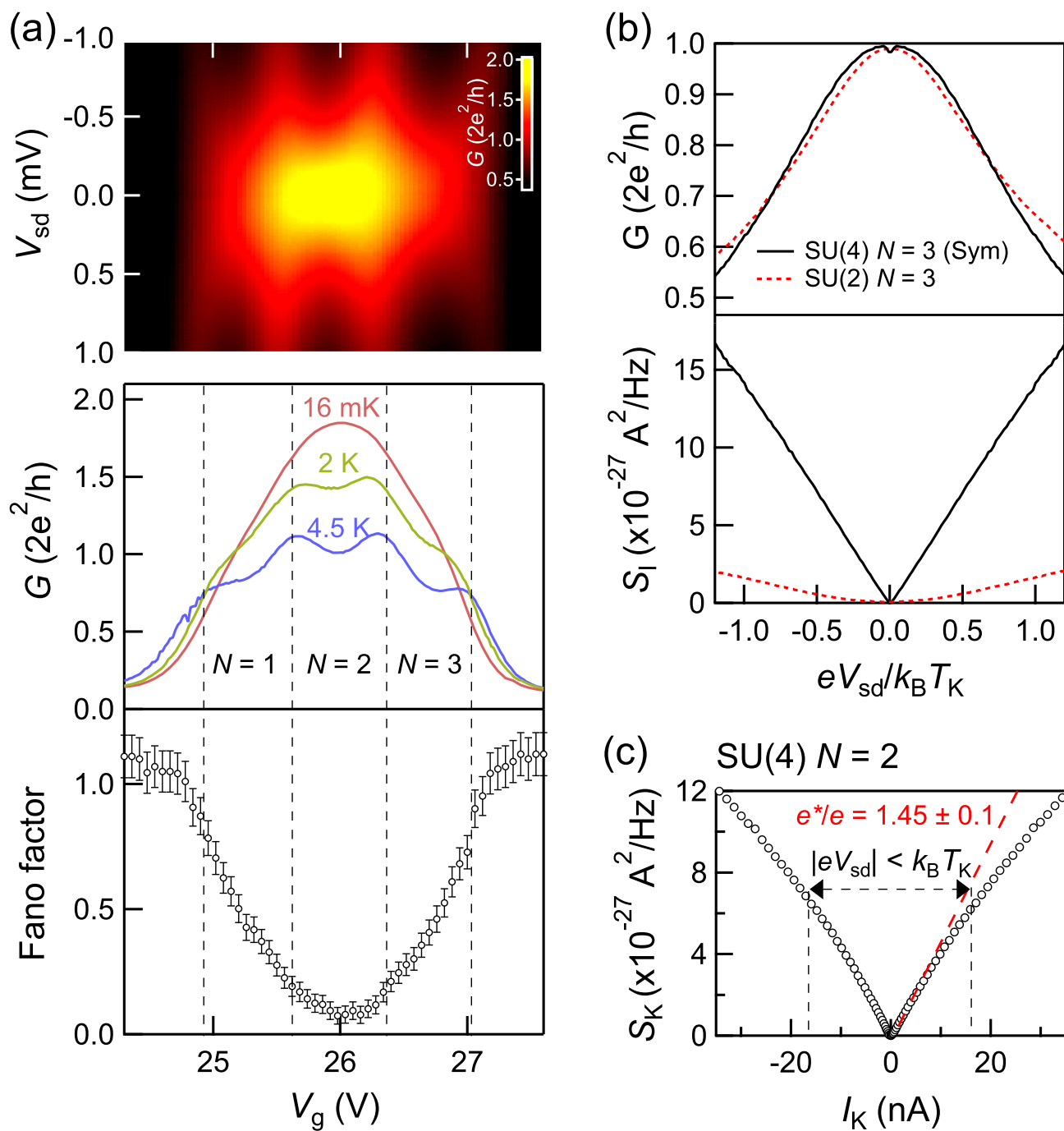


Figure 4

**Figure 4: The SU(4) Kondo state and comparison with the SU(2) symmetry.** **a) top:** 2D plot of the conductance as a function of  $V_{sd}$  and  $V_g$  in the SU(4) state. **Middle:** cross-section of the conductance as a function of the gate voltage at  $V_{sd} = 0$  measured at different temperatures.  $G$  reaches  $1.8 \times \frac{2e^2}{h}$  for the filling  $N = 2$ . **Bottom:** Extracted Fano factor. As expected it varies from  $F \approx 0$  for  $N = 2$  then  $F = 0.5$  for  $N = 1$  and finally  $F = 1$  in the tunneling regime (outside the Kondo ridge). **b)** Comparison of the conductance and the noise for SU(2) Kondo state and SU(4) at filling  $N = 3$ . In both cases the conductance is the same and the two states are not distinguishable. At low voltage, the noise  $S_i$  is qualitatively strongly different. For SU(2) the slope (Fano factor) is close to 0 since the transmission is almost perfect ( $T_1 = 1$ ) whereas the linear part is very important in the SU(4) state since transport occurs through two half transmitting channels ( $T_1 = T_2 = 0.5$ ) yielding  $F = 0.5$ . For clarity, since asymmetry with respect to  $V_{sd}$  appears in the SU(4) state at large voltage, we only compare the symmetrized part of the conductance and the noise for SU(4). We used the definition :  $G^{sym}(V_{sd}) = \frac{G(V_{sd}) + G(-V_{sd})}{2}$  and  $S_i^{sym}(V_{sd}) = \frac{S_i(V_{sd}) + S_i(-V_{sd})}{2}$ . **c)** Kondo excess noise for the SU(4) symmetry at filling  $N = 2$ . A linear fit at low current using formula 2 gives  $e^*/e = 1.45 \pm 0.1$  yielding  $R = 1.35 \pm 0.1$ .